JOC The Journal of Organic Chemistry

Article

pubs.acs.org/joc

Biscembranoids Formed from an α,β-Unsaturated γ-Lactone Ring as a Dienophile: Structure Revision and Establishment of Their Absolute Configurations Using Theoretical Calculations of Electronic Circular Dichroism Spectra

Rui Jia,[†,‡] Tibor Kurtán,[§] Attila Mándi,[§] Xiao-Hong Yan,[†] Wen Zhang,*[,∥] and Yue-Wei Guo*[,†]

[†]State Key Laboratory of Drug Research, Institute of Materia Medica, Chinese Academy of Sciences, Zu Chong Zi Rd. 555, Zhangjiang Hi-Tech Park, Shanghai 201203, P. R. China

[‡]College of Fisheries and Life Science, Water Environment & Ecology Engineer Research Center, Shanghai Ocean University, Shanghai 201306, P. R. China

[§]Department of Organic Chemistry, University of Debrecen, P.O. Box 20, H-4010 Debrecen, Hungary

[∥]Research Center for Marine Drugs, School of Pharmacy, Second Military Medical University, 325 Guo-He Road, Shanghai 200433, P. R. China

Supporting Information

ABSTRACT: Four new biscembranoids, bislatumlides C−F (**1**−**4**), were isolated from the Hainan soft coral *Sarcophyton latum*. Their structures were elucidated by detailed analysis of spectroscopic data and by comparison with reported data of related derivatives, leading to the structure revision of co-occurring bislatumlides A (**5**) and B (**6**) at the C-21 configuration. The absolute configurations of bislatumlides C and E (**1** and **3**) were determined by TDDFT calculations of their solution ECD spectra, allowing the configurational assignment of the related bislatumlides D and F (**2** and **4**) and A and B (**5** and **6**) as well. Bislatumlides A−F (**1**−**6**) represent the only biscembranoids formed by the undescribed coupling pattern of Diels−Alder cycloaddition between the $\Delta^{1(2)}$ double bond involving an α,β-unsaturated γ-lactone ring as a dienophile group and a trisubstituted conjugated $\Delta^{21(34)}/\Delta^{35(36)}$-butadiene moiety. An *endo*-cycloaddition gave **1**, **2**, **5**, and **6**, whereas an *exo*-cycloaddition produced **3** and **4**. This is the first report of *exo*-addition dicembranoids from marine sources and from nature. Bislatumlides C and E (**1**, **3**) could be used as ECD reference compounds in the determination of absolute configuration for related derivatives.

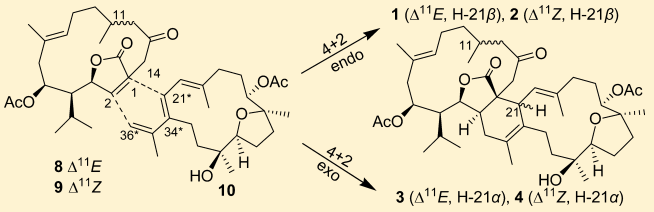

INTRODUCTION

Biscembranoids represent an emerging group of natural products from soft corals of the genera *Sarcophyton*, *Sinularia*, and *Lobophytum* (family Alcyoniidae). More than 60 biscembranoids have been isolated from the three genera to date.[1−14] Most of the biscembranoids are proposed to derive from Diels−Alder addition of two monocembranoid units except for sinulochmodin A, which is likely to be the result of the dimerization of two 18-norcembranoid units by a free radical reaction.[15] Three types of Diels−Alder cycloaddition have been found to form the biscembranoid framework, including cycloaddition between the trisubstituted conjugated $\Delta^{21(34)}/\Delta^{35(36)}$-butadiene moiety of one monomer and the double bonds of $\Delta^{1(14)}$,[1−12] antipodal $\Delta^{14(1)}$,[14] and $\Delta^{1(2)}$,[13] of the other monomer, respectively (see numbering of compounds **8**−**10** in Scheme 1).

Soft corals belonging to the genus *Sarcophyton* are the main source of biscembranoids. Reports of these uncommon tetraterpenoids from the genus *Sarcophyton* have been increasing in the recent years.[1−13] To date, 32 biscembranoids have been isolated from four species of *Sarcophyton* (*S. tortuosum*, *S. latum*, *S. elegans* and *S. glaucum*). Most of the reported biscembranoids exhibited the coupling between the $\Delta^{1(14)}$ double bond activated by a 20-carboxymethyl group and a trisubstituted conjugated $\Delta^{21(34)}/\Delta^{35(36)}$-butadiene moiety, as suggested first for methyl isosartortuoate[1] and then by many other articles.[2−12] The complex and intriguing structures of these dimeric cembranoids have also attracted great interest as targets for total synthesis.[16,17]

In the course of our ongoing search for bioactive secondary metabolites from South China Sea invertebrates,[18−24] the soft coral *S. latum* was collected off the coast of Sanya, Hainan Province. Preliminary investigation of the crude extract of *S. latum* in our laboratory had led to the isolation and structural elucidation of two new cytotoxic biscembranoids, bislatumlides A and B (**5** and **6**), along with one of the proposed monomeric precursors, isosarcophytonolide D (**8**).[13] Bislatumlides A and B

Received: January 14, 2013
Published: February 22, 2013

(**5** and **6**) represent the first examples characterized by an undescribed coupling pattern between the $\Delta^{1(2)}$ double bond involving an α,β-unsaturated γ-lactone ring as a dienophile group and a trisubstituted conjugated $\Delta^{21(34)}/\Delta^{35(36)}$-butadiene moiety. Our further investigation on the less abundant dimeric cembranoids of the crude extract has resulted in the isolation of four new biscembranes, bislatumlides C−F (**1**−**4**), that are structurally related to bislatumlides A and B but display different oxidation patterns at the lower portion of the molecules. Detailed spectroscopic analysis of bislatumlides C−F (**1**−**4**) and bislatumlides A and B (**5** and **6**) resulted in the structural revision of bislatumlides A and B at the C-21 configuration. The absolute configurations of bislatumlides C and E (**1**, **3**) were determined by TDDFT calculations of their solution ECD spectra, affording the configurational assignment of bislatumlides A (**5**), B (**6**), D (**2**) and F (**4**) and their cembrane precursors. Bislatumlides C and E (**1**, **3**) could be used as ECD reference compounds in the determination of absolute configuration for related derivatives. The details of structure elucidation of compounds **1**−**4** are reported herein.

RESULTS AND DISCUSSION

Freshly collected specimens of *S. latum* were kept at −20 °C before extraction. The workup for the extraction and isolation of cembranolides was performed as previously reported.[13] This common procedure yielded four pure compounds, named bislatumlides C−F (**1**−**4**).

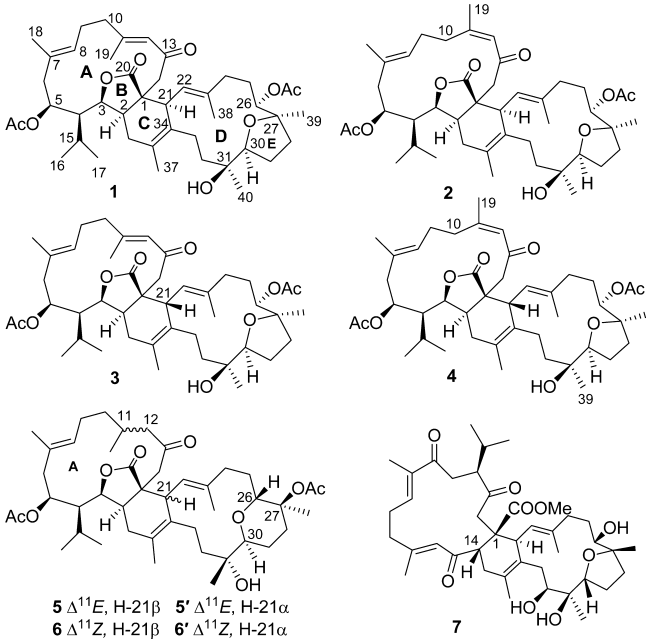

Bislatumlide C (**1**) was obtained as an optically active, UV-absorbing amorphous powder. The molecular formula $C_{44}H_{64}O_9$ was established by HREIMS from the molecular ion at m/z 736.4567 $[M]^+$. The IR spectrum showed the presence of a hydroxyl group (3465 cm^{-1}), ester carbonyl (1736 cm^{-1}) and conjugated carbonyl (1674 cm^{-1}) functionalities. The ^1H NMR spectrum of **1** demonstrated resonances of eight methyls, including two methyls of an isopropyl group (δ 1.08, H_3-17; 1.09, H_3-16; 3H each, d, J = 6.8 Hz), four vinyl methyls (δ 1.66, H_3-18; 1.73, H_3-38; 1.75, H_3-37; 2.11, H_3-19; 3H each, s), and two methyls attached to tertiary-oxygenated carbons (δ 1.07, H_3-40; 1.20, H_3-39; 3H each, s) (Table 1). These data in combination with the appearance of four carbonyl signals (δ 170.4, 5-OAc; 171.1, 26-OAc; 177.7, C-20; 198.0, C-13) in the ^{13}C NMR spectrum (Table 2) suggested bislatumlide C to be an analogue of bislatumides A (**5**) and B (**6**), which had been previously isolated from the same source.[13]

Table 1. ^1H NMR Data of Compounds 1−4 (in $CDCl_3$, 500 MHz)

	1	2	3	4
No.	δ_H, m, J in Hz	δ_H, m, J in Hz	δ_H, m, J in Hz	δ_H, m, J in Hz
2	2.39, m	1.99, m	2.35, m[a]	2.07, m
3	3.83, dd, 10.8, 6.1	3.88,dd,10.5, 4.9	3.71, dd, 11.2, 5.3	3.81, dd, 11.1, 4.8
4	1.46, d, 11.0	1.81, 1H, m	1.42, d, 11.2	1.91, 1H, m
5	4.82, dd, 10.7, 2.7	4.83, dd, 11.2, 3.0	4.80, dd, 8.5, 1.0	4.83, dd, 10.8, 2.3
6α	2.23, m	2.19, m[a]	2.20, m	2.12, m
6β	2.31, m	2.26, m	2.36, m[a]	2.32, m[a]
8	5.11, t, 6.0	5.15, t, 7.5	5.06, m	5.16, t, 7.9
9	2.28, m[a]	2.23, m	2.28, m	2.27, m
10	2.26, m[a]	1.93, m	2.26, m	1.95, m
12	5.85, s	6.0, s	5.97, s	6.0, s
14α	2.52, d, 12.7	2.41, d, 14.5	2.36, d, 11.8	2.72, m
14β	2.78, d, 12.7	3.04, d, 14.5	2.77, d, 11.8	
15	2.17, m	2.18, m[a]	2.15, m	2.23, m
16	1.09,d, 6.8	1.09, d, 6.9	1.11, d, 6.9	1.12, d, 6.9
17	1.08, d, 6.8	1.15, d, 7.0	1.04, d, 7.2	1.18, d, 6.8
18	1.66, s	1.67, s[a]	1.71, s	1.67, s
19	2.11, s	1.87, s	2.09, s	1.90, s
21	3.05, d, 10.7	2.97, d, 10.8	3.45, d, 10.8	3.32, d, 10.4
22	5.59, d, 10.7	5.43, d, 10.8	5.07, d, 10.8	5.02, d, 10.4
24α	2.36, m	2.34, m	2.30, m	2.33, m[a]
24β	1.63, m	1.62, m	1.62, m	1.64, m[a]
25α	1.68, m[a]	1.68, m[a]	1.74, m	1.75, m
25β	2.12, m	2.09, m	1.93, m	
26	4.72, d, 10.7	4.71, d, 10.7	4.66, d, 10.3	4.66, d, 10.5
28α	1.88, m	1.86, m	1.87, m	1.87, m
28β	1.54, m	1.53, m	1.55, m	1.53, m
29α	1.68, m	1.68, m	1.60, m	1.65, m[a]
29β			1.72, m	1.72, m
30	3.90, dd, 10.7, 5.6	3.91, dd, 10.8, 4.7	3.93, dd, 11.4, 5.1	3.93, dd, 11.5, 5.0
32α	1.44, m	1.64, m	1.52, m	1.52, m
32β	1.69, m[a]		1.64, m	
33α	2.35, m	2.45, m	2.66, m	2.86, m
33β	2.03, m	1.97, m	1.85, m	1.85, m
36α	1.86, m	1.89, m	2.50, m	2.38, m
36β	2.28, m	2.28, m	1.60, m	1.61, m
37	1.75, s	1.77, s	1.74, s	1.76, s
38	1.73, s	1.74, s	1.86, s	1.84, s
39	1.20, s	1.19, s	1.19, s	1.19, s
40	1.07, s	1.07, s	0.99, s	1.00, s
5-OAc	2.07, s	2.06, s	2.06, s	2.05, s
26-OAc	2.08, s	2.08, s	2.09, s	2.09, s

[a]Interchangeable values.

A comparison of NMR data of **1** (Tables 1 and 2) with those of **5** immediately revealed similar signals related to rings A, B and C, while signals of rings D and E were significantly different. These facts suggested a similar subunit of rings A, B, and C, and different substitution pattern in rings D and E. In particular, C-26, C-27, and C-30 of **1** resonated at δ_C 74.2, 83.2, and 88.4, whereas the corresponding signals were found at δ_C

dx.doi.org/10.1021/jo400069n | J. Org. Chem. 2013, 78, 3113−3119

Table 2. ^{13}C NMR Data of Compounds 1−4 (in $CDCl_3$, 125 MHz)[a]

	1	2	3	4
No.	δ_C, type	δ_C, type	δ_C, type	δ_C, type
1	52.8, C	52.1, C	53.0, C	51.5, C
2	42.5, CH	42.1, CH	42.8, CH	43.0, CH
3	82.8, CH	83.9, CH	81.9, CH	83.1, CH
4	48.6, CH	47.0, CH	46.8, CH	45.2, CH
5	73.4, CH	72.1, CH	73.8, CH	72.4, CH
6	40.8, CH_2	41.4, CH_2	40.3, CH_2	41.3, CH_2
7	132.6, C	132.0, C	132.6, C	132.0, C
8	126.9, CH	127.6, CH	126.2, CH	127.9, CH
9	24.7, CH_2	25.1, CH_2	24.4, CH_2	25.4, CH_2
10	40.6, CH_2	31.2, CH_2	40.2, CH_2	31.2, CH_2
11	160.6, C	162.1, C	161.3, C	162.1, C
12	125.6, CH	125.0, CH	126.6, CH	125.4, CH
13	198.0, C	198.7, C	198.2, C	198.5, C
14	49.9, CH_2	52.1, CH_2	49.0, CH_2	50.0, CH_2
15	25.8, CH	25.7, CH	25.8, CH	25.7, CH
16	18.2, CH_3	18.4, CH_3	18.0, CH_3	18.4, CH_3
17	25.1, CH_3	24.9, CH_3	24.8, CH_3	24.6, CH_3
18	18.0, CH_3	17.2, CH_3	18.1, CH_3	17.2, CH_3
19	19.3, CH_3	24.6, CH_3	19.0, CH_3	25.0, CH_3
20	177.7, C	179.0, C	180.0, C	182.2, C
21	46.4, CH	47.0, CH	48.2, CH	48.5, CH
22	123.3, CH	123.1, CH	126.0, CH	126.8, CH
23	139.5, C	139.4, C	140.5, C	140.2, C
24	32.7, CH_2	32.7, CH_2	32.8, CH_2	32.8, CH_2
25	29.6, CH_2	29.8, CH_2	31.5, CH_2	29.4, CH_2
26	74.2, CH	74.2, CH	73.8, CH	74.0, CH
27	83.2, C	83.2, C	83.3, C	83.4, C
28	36.8, CH_2	36.7, CH_2	36.7, CH_2	36.7, CH_2
29	27.1, CH_2	27.2, CH_2	27.1, CH_2	27.2, CH_2
30	88.4, CH	88.4, CH	88.7, CH	88.8, CH
31	73.7, C	73.8, C	74.3, C	74.3, C
32	33.8, CH_2	33.6, CH_2	31.5, CH_2	32.2, CH_2
33	26.3, CH_2	26.6, CH_2	26.6, CH_2	26.6, CH_2
34	126.6, C	126.8, C	125.8, C	126.4, C
35	135.8, C	135.1, C	138.5, C	137.6, C
36	34.1, CH_2	34.4, CH_2	34.3, CH_2	34.4, CH_2
37	20.0, CH_3	20.1, CH_3	21.1, CH_3[b]	21.1, CH_3[b]
38	20.5, CH_3	20.6, CH_3	20.9, CH_3	20.9, CH_3
39	20.9, CH_3	20.9, CH_3	20.7, CH_3	20.7, CH_3
40	22.9, CH_3	22.8, CH_3	21.8, CH_3	21.8, CH_3
5-OAc	170.4, C; 21.3, CH_3	170.4, C; 21.3, CH_3	170.5, C; 21.2, CH_3[b]	170.5, C; 21.2, CH_3[b]
26-OAc	171.1, C; 21.3, CH_3	171.2, C; 21.3, CH_3	171.1, C; 21.3, CH_3	171.1, C; 21.3, CH_3

[a]The assignments made by DEPT, $^1H-^1H$ COSY, HMQC and HMBC experiments. [b]Interchangeable values.

85.6, 69.9, and 68.1 in **5**, respectively. The chemical shifts of the above three carbon atoms in **1** were in good agreement with those in bisglaucumlide G (**7**)[11] and its analogues ximaolides C and D,[9] suggesting the presence of a tetrahydrofuran ring E in **1** instead of the tetrahydropyran ring in **5**. The proposed planar structure of **1** was further confirmed by detailed analysis of the 2D NMR data as shown in Figure 1.

The *E* geometry of the $\Delta^{7(8)}$, $\Delta^{11(12)}$, $\Delta^{22(23)}$ double bonds in **1** was deduced from the ^{13}C NMR data of related olefinic methyl groups (Table 2)[13,25,26] and further confirmed by the NOESY experiment. The relative configuration of chirality centers in rings A and B were proven the same as those of **5** because of the distinct NOE correlations of H-3 with H-2, H-4 and H-5, while the relative configuration of the chirality centers C-26, C-27 and C-30 were assigned the same as those of **7** because of the diagnostic NOEs between signals for H-30 and H_3-39, H-30 and H-28α, and between H-26 and H-28β . The NOE correlation between H_3-40 and H-30 suggested the α orientation of H_3-40. The *cis* relative configuration of the two chirality centers (C-2 and C-21) established during the Diels−Alder cycloaddition of the monomers was determined on the ground of the NOE correlation between H-21 and H-2. Moreover, NOE correlations between H-21 and H-33α, and H-33α and H_3-40 allowed correlating the relative configuration of the two subunits. Thus (1*R**,2*S**,3*R**,4*R**,5*R**,21*R**,26*S**,27*S**,30*R**,31*R**) relative configuration was established, which was also supported by similar chemical shifts and coupling patterns in the ^1H NMR spectra of **7** and its analogues for ring E.[9,11]

Bislatumlide D (**2**) was also obtained as a UV-absorbing, optically active solid. Its molecular formula of $C_{44}H_{64}O_9$, deduced from the MS and NMR spectra, was the same as that of **1**. The NMR data of **2** were highly compatible with those of **1**. Detailed analysis of 1D and 2D NMR spectra of **2** revealed the same gross structure as that of **1**. However, the signal of the C-19 in **2** was remarkably downfield-shifted (δ 19.3 in **1**, 24.6 in **2**), whereas that of C-10 was remarkably upfield-shifted (δ 40.6 in **1**, 31.2 in **2**), indicating a *Z* geometry of $\Delta^{11(12)}$ in **2** in contrast to the 11*E* double bond in **1**. The conclusion was further supported by a strong NOE correlation between H-12 and H_3-19 signals for **2**. Compound **2** was thus determined as the 11*Z* isomer of **1**.

Bislatumlide E (**3**) had the same molecular formula as that of **1** as indicated by MS and NMR spectra. The ^1H and ^{13}C NMR data of **3** closely resembled those of **1** (Tables 1 and 2). The only difference was recognized in the signals of ring C. In particular, the ^1H NMR for H-21 was sharply downfield-shifted (δ 3.45 for **3** and δ 3.05 for **1**), whereas H-22 was remarkably upfield-shifted (δ 5.07 for **3** and δ 5.59 for **1**). This fact suggested different configurations of H-21 in the two compounds. The distinct NOE effect between H-21 and H-33β protons and the absence of the NOE correlations between

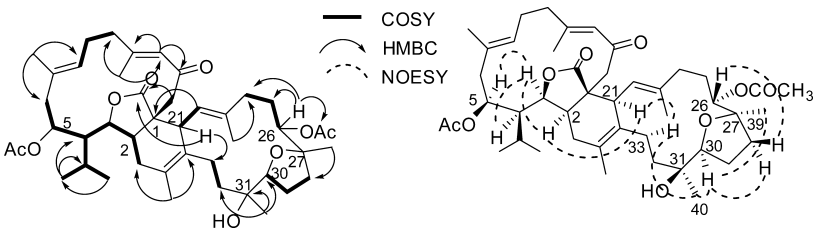

Figure 1. The $^1H-^1H$ COSY, selected HMBC, and key NOESY correlations of **1**.

dx.doi.org/10.1021/jo400069n | J. Org. Chem. 2013, 78, 3113−3119

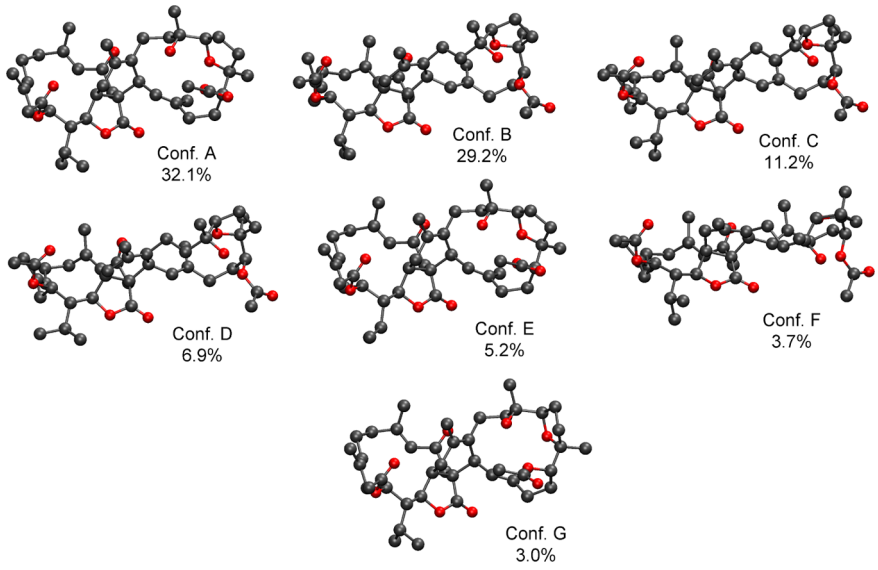

Figure 2. Computed DFT-optimized conformers of (1*R*,2*S*,3*R*,4*R*,5*R*,7*E*,11*E*,21*R*,22*E*,26*S*,27*S*,30*R*,31*R*,34*Z*)-**1** and their populations (hydrogen atoms are not displayed).

H-21 and H-2 signals in **3** supported the above assignment. The relative configurations at other chirality centers of **3** were proven the same as those of **1** by detailed analysis of 1D and 2D NMR spectra. The structure of **3** was therefore determined as the C-21 epimer of **1**; i.e., the Diels−Alder cycloaddition produced *trans* relative configuration of H-2 and H-21 in **3**.

Bislatumlide F (**4**) was readily recognized as an analogue of **3**. Its ^{1}H and ^{13}C NMR data were similar to those of **3** except for those signals assigned to C-10 and C-19. The ^{13}C resonance for C-19 was shifted downfield from δ 19.0 in **3** to 25.0 in **4**, whereas that for C-10 was shifted upfield from δ 40.2 in **3** to 31.2 in **4**. The observations led to the assignment of an 11*Z* double bond in **4**. The distinct NOE correlation between H-12 and H_3-19 signals in the NOESY spectrum of **4** supported the above conclusion. Compound **4** was therefore determined as the 11*Z* isomer of **3**.

With the completion of the structure elucidation of bislatumlides C−F, it is interesting to note that, apparently, the structures **1** and **2** differ from **3** and **4** only in the relative configuration of H-21 (α for **1** and **2** and β for **3** and **4**). However, this small structural difference has caused significant differences in the chemical shift values of both H-21 and H-22. Thus, the δ values of H-21β (δ 3.45 in **3** and 3.32 in **4**) were remarkably shifted downfield with respected to those of H-21α (3.05 in **1** and 2.97 in **2**), whereas H-22 of **3** and **4** were resonated in upfield respect to that of **1** and **2** (δ 5.07 and 5.02 in **3** and **4** vs δ 5.59 and 5.43 in **1** and **2**, respectively). Meanwhile, the ^{13}C NMR signals for C-22 in **1** and **2** (δ 123.3 and 123.1) were also reasonably upfield-shifted in comparison with those in **3** and **4** (δ 126.0 and 126.8) (Tables 1 and 2) because of the γ-gauche effect.[27−30] In light of these observations, it raises a necessity to check the configuration of H-21 in both bislatumlides A and B (**5** and **6**). Because the ^{1}H NMR chemical shift values of H-21 (δ 3.09 in **5** and 2.85 in **6**) and H-22 (δ 6.15 in **5** and 5.96 in **6**)[13] are more similar to those of **1** and **2**, instead of those **3** and **4** (Table S1 in the Supporting Information), the previously assigned structures **5** and **6** should be revised as **5′** and **6′**, respectively. The observed ^{13}C NMR shift values for C-22 in both **5** and **6** (δ 121.3 in **5** and 121.1 in **6**)[13] further supported the above conclusion (Table S2 in the Supporting Information).

The configurational assignment of biscembranoids by circular dichroism methods is a challenging task considering the conformational flexibility and large molecular weight of these derivatives. However, once achieved, the comparison of the ECD spectra of related derivatives provides a straightforwardly comparative method for determination of absolute configuration. Recently, the convenient solid-state TDDFT-ECD method has been used to determine the absolute configuration of the biscembranoid derivative, ximaolide A, which also afforded the configurational assignment of related derivatives ximaolides B−G.[31] Since the relative solid-state X-ray geometry of bislutamlide C (**1**) was not available, the solution conformers and their ECD spectra had to be calculated by DFT methods. The initial MMFF conformational analysis of the arbitrarily chosen (1*R*,2*S*,3*R*,4*R*,5*R*,21*R*,26*S*,27*S*,30*R*,31*R*)-**1** provided 78 conformers, the DFT reoptimization of which produced 7 conformers above 2% population (Figures 2 and S1 in the Supporting Information). In conformer A (32.1%), the central cyclohexene ring adopted a twist boat conformation with *axial* H-2 and *equatorial* H-21, and conformer E (5.2%) and G (3.0%) showed similar geometries. The cyclohexene ring of conformer F (3.7%) had also a twist boat conformation but with *equatorial* H-2 and *axial* H-21. In the slightly different conformers B (29.2%), C (11.2%) and D (6.9%), the cyclohexene ring had a half-chair conformation with *cis* 1,3-*diaxial* arrangement of H-2 and H-21. These latter conformers are responsible for the characteristic NOE effect between H-2 and H-21. The conformation of the central cyclohexene ring is clearly decisive on the relative arrangement of the two macrocycles, and thus it also influences the optical parameters. The experimental solution ECD spectrum of bislutamlide C (**1**) showed a broad negative Cotton effect (CE) at 254 nm and a more intense positive one at 213 nm (Figure 3). The Boltzmann-weighted TDDFT ECD spectra of conformers A−G of (1*R*,2*S*,3*R*,4*R*,5*R*,21*R*,26*S*,27*S*,30*R*,31*R*)-**1** produced a mirror image ECD curve of the experimental spectrum with various functionals (B3LYP, BH&HLYP, PBE0) and 6-311G(d,p) basis set (Figure 3). Thus the absolute configuration

dx.doi.org/10.1021/jo400069n | *J. Org. Chem.* 2013, 78, 3113−3119

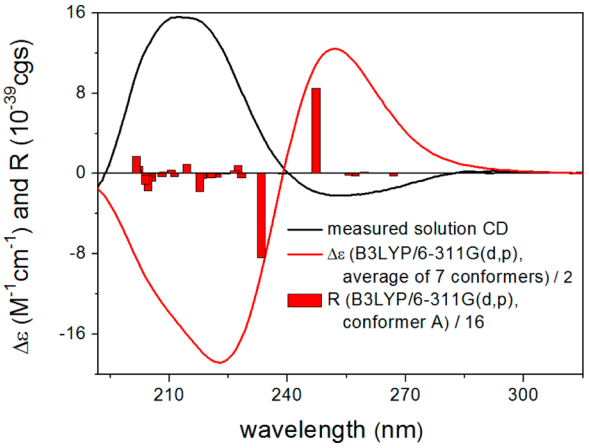

Figure 3. Experimental solution (acetonitrile, black curve) ECD spectrum of bislutamlide C (**1**) compared with the computed B3LYP/6-311G(d,p) spectrum (red) of (1*R*,2*S*,3*R*,4*R*,5*R*,21*R*,26*S*,27*S*,-30*R*,31*R*)-**1** obtained as the Boltzmann-weighted average of conformers A−G. Bars represent rotational strength of the lowest-energy conformer.

of bislatumlide C (**1**) was determined as (+)-(1*S*,2*R*,3*S*,4*S*,5*S*,21*S*,26*R*,27*R*,30*S*,31*S*). The ECD calculation also revealed that although the two observed ECD bands derive from several overlapping transitions, there are two intense oppositely signed ECD transitions (rotatory strengths), which are dominant. Thus the broad negative CE at 254 nm is governed by the enone $\pi-\pi^*$ transition with some charge-transfer contribution, while the 213 nm positive CE derives from the $\pi-\pi^*$ transition of the two isolated $\Delta^{22(23)}$ and $\Delta^{34(35)}$ double bonds. The ECD spectrum of bislatumlides A (**5**′), B (**6**′), and D (**2**) showed the same pattern as that of bislatumlide C (**1**), suggesting that their chirality centers have the same absolute configuration.

Despite the apparently minor change in stereochemistry, bislatumlide E (**3**) showed a significantly different ECD spectrum from that of bislatumlide C (**1**). It had a strong negative CE at 209 nm, a weak positive one at 235 nm, and a broad negative band at 264 nm. In order to reveal the origin of the different ECD spectrum and confirm the absolute configuration, the solution TDDFT-ECD approach was also applied to bislatumlide E (**3**). The DFT reoptimization of the initial 87 MMFF conformers provided 4 major conformers above 2% populations (Figures 4 and S2 in the Supporting Information). In conformer A (52.9%), C (13.0%) and D (3.1%) the cyclohexene ring adopted a twist boat conformation with *trans diaxial* orientation of H-2 and H-21, while in conformer B (24.4%) the cyclohexene ring flipped to the other twist boat conformation pushing H-2 and H-21 into *trans equatorial* orientation and hence changing the relative arrangement of the two macrocycles as well. Thus when comparing the conformers of **1** and **3**, it is clear that the inversion of H-21 had a significant effect on the conformational ensembles, since the half-chair conformation of the cyclohexene ring was dominant for **1** (totalling 47.3%), and two forms of its twist boat conformation were identified for **3**. These differences are reflected in their different optical parameters. The Boltzmann-weighted TDDFT ECD spectra of conformers A−D of (1*R*,2*S*,3*R*,4*R*,5*R*,21*S*,26*S*,27*S*,30*R*,31*R*)-**3** produced a mirror image ECD curve of the experimental spectrum (Figure 5) determining the absolute configuration of bislatumlide E (**3**) as (−)-(1*S*,2*R*,3*S*,4*S*,5*S*,21*R*,26*R*,27*R*,30*S*,31*S*).

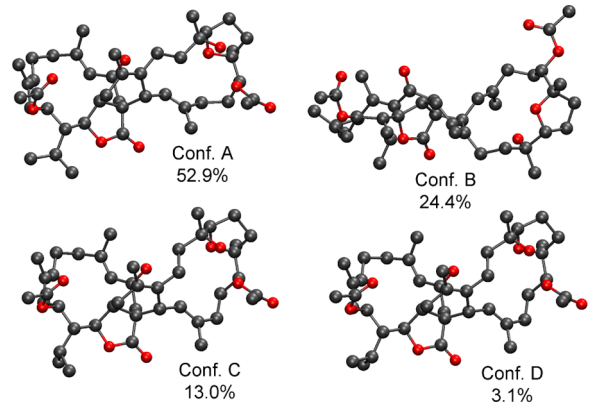

Figure 4. Computed DFT optimized conformers of (1*R*,2*S*,3*R*,4*R*,5*R*,7*E*,11*E*,21*S*,22*E*,26*S*,27*S*,30*R*,31*R*,34*Z*)-**3** and their populations (hydrogen atoms are not displayed).

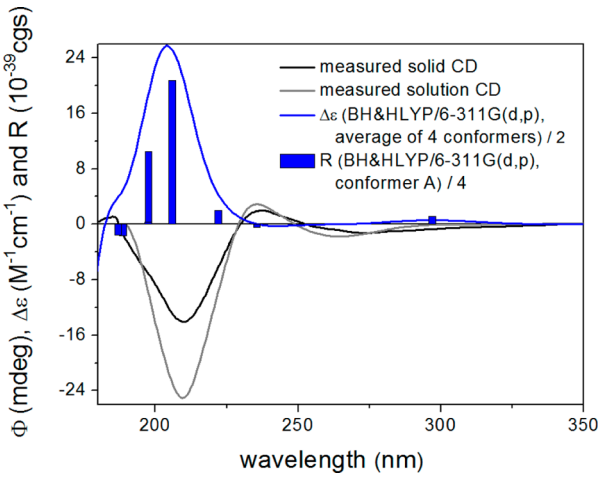

Figure 5. Solid and solution ECD spectrum of bislatumlide E (**3**) in acetonitrile compared with the B3LYP/6-311G(d,p) computed Boltzmann-weighted ECD spectrum of (1*R*,2*S*,3*R*,4*R*,5*R*,21*S*,26*S*,27*S*,-30*R*,31*R*)-**3**. Bars represent the rotatory strength of the lowest-energy conformer.

The inspection of the computed molecular orbitals of the rotatory strengths showed that the 264 nm negative CE is governed by the enone n−π^* transition, while the intense negative 209 nm CE derives from the sum of a negative enone $\pi-\pi^*$ and a charge-transfer transition. The solid-state microcrystalline ECD spectral data of **3** were also recorded as a KCl pellet, which were found to be near identical with that of the solution one, proving that the solid-state conformer is the dominant one in solution as well (Figure 5). The ECD spectrum of **4** showed the same pattern as that of **3** with more intense CEs confirming the homochirality of the two derivatives.

Similarly to bislatumlides A and B, the plausible biogenetic pathway of compounds **1**−**4** involves a nondiastereoselective Diels−Alder reaction of a diene (**10**) and a dienophile (**8** or **9**) as shown in Scheme 1. Isosarcophytonolide D (**8**),[13] isolated earlier from the same source, may act as dienophile to form biscembranes **1** and **3** in a Diels−Alder reaction with the diene **10** following *endo* or *exo* selectivity, respectively. The cyloaddition is supposed to occur between the $\Delta^{1(2)}$ double bond of the unsaturated lactone moiety of **8** and $\Delta^{21(34),35(36)}$ diene functionality of **10** as described previously for

dx.doi.org/10.1021/jo400069n | J. Org. Chem. 2013, 78, 3113−3119

Scheme 1. Plausible Diels-Alder Reactions Leading to Compounds 1−4

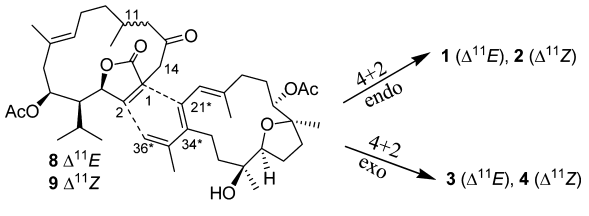

10

*formally numbered according to **1**- **4**

bislatumlides A and B.[10] To our knowledge, this is the second report of cembranoid dimers formed by the coupling of an α,β-unsaturated γ-lactone ring, and almost all the previously reported cembrane dienophile precursors had a $\Delta^{1(14)}$ double bond (according to the numbering of **8**), whereas in the present case, the conjugating double bond of **8** had $\Delta^{1(2)}$ position. The endo products of the Diels−Alder reaction (**1**, **2**) had *cis* relative configuration of the new chirality centers H-2 and H-21, while the *exo* products (**3**, **4**) had *trans* orientation of H-2 and H-21. The stereochemical study of biscembranes **1**−**4** also allows the configurational assignment of the previously reported dienophiles isosarcophytonolide D (**8**)[13] and sarcophytonolide A (**9**),[21] and the diene **10**, which has not been reported yet. The absolute configuration of bislatumlides A and B could be also assigned, as well as their diene monomer isolated and reported earlier with only relative configuration.[32,33]

Since both bislatumlides A and B exhibited interesting cytotoxicities against several tumor cell lines,[13] compounds **1**−**4** were also tested for cytotoxicity against A-549 and HL-60 tumor cell lines; unfortunately, they were all inactive at a concentration of 20 μg/mL. Compounds **1**−**4** were also inactive in other bioassays; they showed no antibacterial and anti-inflammatory activities.

EXPERIMENTAL SECTION

General Experimental Procedures. Commercial Si gel (200−300 and 400−600 mesh) was used for column chromatography, and precoated Si gel plates (G60 F-254) were used for analytical TLC. Sephadex LH-20 gel was used for column chromatography. NMR spectra were at 293 K. Chemical shifts are reported in parts per million (δ), using the residual $CHCl_3$ signal (δ_H 7.26 ppm) as an internal standard for ^{1}H NMR and $CDCl_3$ (δ_C 77.0 ppm) for ^{13}C NMR; coupling constant (J) is in Hz. Infrared spectra were recorded in thin polymer films. For the solid-state circular dichroism (CD) protocol, see ref 31. The mass spectra and high resolution mass spectra were performed on a double-focusing magnetic mass spectrometer equipped with an electron ionization source. Semipreparative RP-HPLC was performed using a refractive index detector and a column with 5 μm, 250 × 10 mm size.

Biological Material. Specimens of *S. latum*, identified by Prof. R.-L. Zhou of South China Sea Institute of Oceanology Chinese Academy Sciences, were collected along the coast of Ximao island, Sanya, Hainan Province, China, in December 2002, at a depth of −20 m and were frozen immediately after collection. A voucher specimen is available at the Shanghai Institute of Materia Medica, CAS (No. 02HN103).

Extraction and Isolation. The frozen animals (68 g, dry weight) were cut into pieces and extracted exhaustively with acetone at rt (3 × 1.5 L). The organic extract was evaporated to give a residue, which was partitioned between Et_2O and H_2O. The Et_2O solution was concentrated under reduced pressure to give a dark brown residue (3.2 g), which was fractionated by gradient Si gel column chromatography (0−100% acetone in light petroleum ether) yielding a mixture showing interesting yellow TLC spots after spraying with H_2SO_4 [R_f 0.4−0.5 (PE/CH_3COCH_3, 2:1)]. The fraction was further purified by RP-HPLC (MeCN/H_2O, 4:1; 2.0 mL/min) to give four pure compounds **1** (3.6 mg, 17 min), **2** (4.7 mg, 25 min), **3** (2.8 mg, 20 min), and **4** (2.5 mg, 29 min).

*Bislatumlide C (**1**).* White amorphous powder: $[\alpha]^{20}_D$ +35.2 (c 0.53, $CHCl_3$); ECD (MeCN, λ_{max} [nm] ($\Delta\varepsilon$), c = 1.19 × 10^{-4}) 254 (−2.19), 213 (15.58), negative below 195 nm; ECD (70 μg **1** in 250 mg KCl, λ_{max} [nm] ($\Delta\varepsilon$) 254 (−3.38), 218 (17.42); UV (MeOH) λ_{max} (log ε) 246 (3.2) nm; IR (Film) ν_{max} 3465, 2937, 1736, 1674, 1606, 1243, 1038, 757 cm^{-1}; ^{1}H and ^{13}C NMR, see Tables 1 and 2; MS(EI) m/z 736 $[M]^+$ (14), 718 (100), 676 (18), 658 (54), 633 (26), 362 (98), 344 (50), 284 (33), 159 (52), 133 (86); HRMS(EI) $[M]^+$ m/z 736.4567 (calcd for $C_{44}H_{64}O_9$, 736.4551).

*Bislatumlide D (**2**).* White amorphous powder: $[\alpha]^{20}_D$ + 40.3 (c 0.35, $CHCl_3$); ECD (MeCN, λ_{max} [nm] ($\Delta\varepsilon$), c = 9.20 × 10^{-5}) 261 (−8.96), 235sh (6.10), 217 (21.09). ECD (61 μg **2** in 250 mg KCl, λ_{max} [nm] ($\Delta\varepsilon$) 270 (−4.58), 241sh (5.62), 220 (25.34); UV (MeOH) λ_{max} (log ε) 242 (3.1) nm; IR (Film) ν_{max} 3468, 2935, 1737, 1670, 1603, 1043, 758 cm^{-1}; ^{1}H and ^{13}C NMR, see Tables 1 and 2; MS(EI) 736 $[M]^+$ (4), 718 (7), 676 (5), 658 (8), 362 (100), 344 (25), 284 (10), 159 (13), 133 (24), 93 (13); HRMS(EI) $[M]^+$ m/z 736.4542 (calcd for $C_{44}H_{64}O_9$, 736.4551).

*Bislatumlide E (**3**).* White amorphous powder: $[\alpha]^{20}_D$ −56.0 (c 0.17, $CHCl_3$); ECD (MeCN, λ_{max} [nm] ($\Delta\varepsilon$), c = 9.41 × 10^{-5}) 276sh (−1.20), 264 (−1.83), 244sh (1.87), 235 (3.14), 209 (−26−15). ECD (44 μg **3** in 250 mg KCl, λ_{max} [nm] ($\Delta\varepsilon$) 271 (−1.32), 236 (2.29), 209 (−14.78); UV (MeOH) λ_{max} (log ε) 245 (2.8) nm; IR (Film) ν_{max} 3467, 2940, 1732, 1672, 1605, 1240, 1040, 762 cm^{-1}; ^{1}H and ^{13}C NMR, see Tables 1 and 2; MS(EI) 736 $[M]^+$ (38), 718 (83), 676 (28), 658 (51), 633 (32), 579 (39), 497 (26), 362 (90), 344 (25), 133 (100); HRMS(EI) $[M]^+$ m/z 736.4565 (calcd for $C_{44}H_{64}O_9$, 736.4551).

*Bislatumlide F (**4**).* White amorphous powder: $[\alpha]^{20}_D$ −74.0 (c 0.17, $CHCl_3$); ECD (MeCN, λ_{max} [nm] ($\Delta\varepsilon$), c = 1.01 × 10^{-4}) 277sh (−7.03), 262 (−11.97), 241sh (5.04), 234 (10.22), 211 (−40.68), positive below 195 nm; ECD (43 μg **4** in 252 mg KCl, λ_{max} [nm] ($\Delta\varepsilon$) 286sh (−1.89), 274 (−3.27), 248sh (4.11), 235 (8.73), 211 (−26.26); UV (MeOH) λ_{max} (log ε) 241 (4.6) nm; IR (Film) ν_{max} 3470, 2934, 1738, 1670, 1602, 1042, 755 cm^{-1}; ^{1}H and ^{13}C NMR, see Tables 1 and 2; MS(EI) 736 $[M]^+$ (9), 718 (6), 676 (6), 658 (7), 362 (100), 344 (8), 284 (12), 159 (13), 133 (21), 93 (11); HRMS(EI) $[M]^+$ m/z 736.4554 (calcd for $C_{44}H_{64}O_9$, 736.4551).

*Bislatumlide A (**5**).*[13] ECD (MeCN, λ_{max} [nm] ($\Delta\varepsilon$), c = 1.04 × 10^{-4}) 262 (−3.05), 225 (3.92), negative below 207 nm.

*Bislatumlide B (**6**).*[13] ECD (MeCN, λ_{max} [nm] ($\Delta\varepsilon$), c = 1.39 × 10^{-4}) 263 (−3.89), 229 (4.69), negative below 211 nm.

Computational Section. Mixed torsional/low mode conformational searches were carried out by means of the Macromodel 9.9.223[34] software using Merck Molecular Force Field (MMFF) with implicit solvent model for chloroform and 21 kJ/mol energy window. Geometry reoptimizations at B3LYP/6-31G(d) in gas phase followed by TDDFT calculations using various functionals (B3LYP, BH&HLYP, PBE0) and 6-311G(d,p) basis set were performed by the Gaussian 09[35] package. Boltzmann distributions were estimated from the B3LYP/6-31G(d) energies. ECD spectra were generated as the sum of Gaussians[36] with 3000 and 2100 cm^{-1} half-height width (corresponding to ca. 14 and 10 nm at 215 nm), using dipole-velocity computed rotational strengths for conformers above 2%. The VMD[37] and GaussView[38] software packages were used for visualization of the results.

ASSOCIATED CONTENT

Supporting Information

MS, HRMS, one- and two- dimensional NMR spectra for compounds **1**−**4**, and atom coordinates and absolute energies of the computed structures. This material is available free of charge via the Internet at http://pubs.acs.org.

dx.doi.org/10.1021/jo400069n | J. Org. Chem. 2013, 78, 3113−3119

AUTHOR INFORMATION

Corresponding Author

*E-mail: ywguo@mail.shcnc.ac.cn, wenzhang1968@163.com.

Notes

The authors declare no competing financial interest.

ACKNOWLEDGMENTS

This research was financially supported by the National Marine "863" Project (No. 2013AA092902 and 2011AA09070102), the Natural Science Foundation of China (Nos. 21072204 and 21021063), and partially funded by the STCSM International Cooperation Project between SIMM/China and ICB/Italy (No. 10540702900), the EU Seventh Framework Programme-IRSES Project (2010-2014), the SKLDR/SIMM Projects (Nos. SIMM1105KF-04 and SIMM1106KF-11), and CAS Grants (Nos. KSCX2-YW-R-18 and KSCX2-EW-R-15). T.K. and A.M. thank the Hungarian National Research Foundation for financial suppport (OTKA K105871, K81701) and the National Information Infrastructure Development Institute (NIIFI 10038). We acknowledge the collection of biological material by Dr. E. Mollo of ICB-CNR, Italy. We also indebted to Prof. J. Ding and H.-Y. Zhang for the bioassay help.

REFERENCES

(1) Su, J.-Y.; Long, K.-H.; Peng, T.-S. *J. Am. Chem. Soc.* **1986**, *108*, 177−178.

(2) Su, J.-Y.; Long, K.-H.; Peng, T.-S.; Zeng, L.-M. *Sci. China, Ser. B: Chem.* **1988**, *31*, 1172−1184.

(3) Kusumi, T.; Igari, M.; Ishitsuka, M. O.; Ichikawa, A.; Itezono, Y.; Nakayama, N.; Kakisawa, H. J. *J. Org. Chem.* **1990**, *55*, 6286−6289.

(4) Ishitsuka, M. O.; Kusumi, T.; Kakisawa, H. *Tetrahedron Lett.* **1991**, *32*, 6595−6596.

(5) Leone, P. A.; Caroll, A. R.; Coll, J. C.; Meehan, G. V. *J. Nat. Prod.* **1993**, *56*, 521−526.

(6) Feller, M.; Rudi, A.; Berer, N.; Goldberg, I.; Stein, Z.; Benayahu, Y.; Schleyer, M.; Kashman, Y. *J. Nat. Prod.* **2004**, *67*, 1303−1308.

(7) Zeng, L.-M.; Lan, W.-J.; Su, J.-Y.; Zhang, G.-W.; Feng, X.-L.; Liang, Y.-L.; Yang, X. P. *J. Nat. Prod.* **2004**, *67*, 1915−1918.

(8) Iwagawa, T.; Hashimoto, K.; Okamura, H.; Kurawai, J.; Nakatani, M.; Hou, D. X.; Fujii, M.; Doe, M.; Morimoto, Y.; Takemura, K. *J. Nat. Prod.* **2006**, *69*, 1130−1133.

(9) Jia, R.; Guo, Y.-W.; Chen, P.; Yang, Y.-M.; Mollo, E.; Gavagnin, M.; Cimino, G. *J. Nat. Prod.* **2007**, *70*, 1158−1166.

(10) Jia, R.; Guo, Y.-W.; Mollo, E.; Gavagnin, M.; Cimino, G. *Helv. Chim. Acta* **2008**, *91*, 2069−2074.

(11) Iwagawa, T.; Hashimoto, K.; Yokogawa, Y.; Okamura, H.; Nakatani, M.; Doe, M.; Morimoto, Y.; Takemura, K. *J. Nat. Prod.* **2009**, *72*, 946−949.

(12) Bishara, A.; Rudi, A.; Benayahu, Y.; Kashman, Y. *J. Nat. Prod.* **2007**, *70*, 1951−1954.

(13) Yan, X.-H.; Gavagnin, M.; Cimino, G.; Guo, Y.-W. *Tetrahedron Lett.* **2007**, *48*, 5313−5316.

(14) Yan, P.-C.; Lv, Y.; Ofwegen, L. V.; Proksch, P.; Lin, W.-H. *Org. Lett.* **2010**, *12*, 2484−2487.

(15) Tseng, Y. J.; Ahmed, A. F.; Dai, C. F.; Chiang, M. Y.; Sheu, J. H. *Org. Lett.* **2005**, *7*, 3813−3815.

(16) Ichige, T.; Okano, Y.; Kanoh, N.; Nakata, M. *J. Org. Chem.* **2009**, *74*, 230−243.

(17) Ichige, T.; Okano, Y.; Kanoh, N.; Nakata, M. *J. Am. Chem. Soc.* **2007**, *129*, 9862−9863.

(18) Wang, Z.; Zhang, H.; Yuan, W.; Gong, W.; Tang, H.; Liu, B.; Yi, Y.; Zhang, W. *Food Chem.* **2011**, *132*, 295−300.

(19) Li, C.; La, M.-P.; Sun, P.; Kurtán, T.; Mándi, A.; Tang, H.; Liu, B.-S.; Yi, Y.; Zhang, W. *Mar. Drugs* **2011**, *9*, 1403−1418.

(20) Li, C.; La, M.-P.; Li, L.; Li, X.-B.; Tang, H.; Liu, B.-S.; Krohn, K.; Sun, P.; Yi, Y.; Zhang, W. *J. Nat. Prod.* **2011**, *74*, 1658−1662.

(21) Jia, R.; Guo, Y.-W.; Mollo, E.; Gavagnin, M.; Cimino, G. *Helv. Chim. Acta* **2005**, *88*, 1028−1033.

(22) Li, L.; Sheng, L.; Wang, C.-Y.; Zhou, Y.-B.; Huang, H.; Li, X.-B.; Li, J.; Mollo, E.; Gavagnin, M.; Guo, Y.-W. *J. Nat. Prod.* **2011**, *74*, 1902−1907.

(23) Li, Y.; Carbone, M.; Vitale, R. M.; Sicilia, P. G.; Mollo, E.; Nappo, M.; Cimino, G.; Guo, Y. W.; Gavagnin, M. *J. Nat. Prod.* **2010**, *73*, 133−138.

(24) Yan, X.-H.; Liu, H. L.; Huang, H.; Li, X.-B.; Guo, Y.-W. *J. Nat. Prod.* **2011**, *74*, 175−180.

(25) Kusumi, T.; Igari, M.; Ishitsuka, M. O.; Ichikawa, A.; Itezono, Y.; Nakayama, N.; Kakisawa, H. *J. Org. Chem.* **1990**, *55*, 6286−6289.

(26) Abraham, R. J.; Monasterios, J. R. *J. Chem. Soc., Perkin. Trans. II* **1974**, 662−665.

(27) Barfield, M.; Yamamura, S. H. *J. Am. Chem. Soc.* **1990**, *112*, 4747−4758.

(28) Li, S.; Chesnut, D. B. *Magn. Reson. Chem.* **1985**, *23*, 625−638.

(29) Seidman, K.; Maciel, G. E. *J. Am. Chem. Soc.* **1977**, *99*, 659−671.

(30) Grant, D. M.; Cheney, B. V. *J. Am. Chem. Soc.* **1967**, *89*, 5315−5318.

(31) Kurtán, T.; Jia, R.; Li, Y.; Pescitelli, G.; Guo, Y.-W. *Eur. J. Org. Chem.* **2012**, 6722−6728.

(32) Wang, S.-K.; Hsieh, M.-K.; Duh, C.-Y. *Mar. Drugs* **2012**, *10*, 1433−1444.

(33) Yan, P.; Deng, Z.; van Ofwegen, L.; Proksch, P.; Lin, W. *Mar. Drugs* **2010**, *8*, 2837−2848.

(34) MacroModel, Schrödinger LLC, to be found under http://www.schrodinger.com/productpage/14/11/, 2012.

(35) Frisch, M. J.; Trucks, G. W.; Schlegel, H. B.; Scuseria, G. E.; Robb, M. A.; Cheeseman, J. R.; Scalmani, G.; Barone, V.; Mennucci, B.; Petersson, G. A.; Nakatsuji, H.; Caricato, M.; Li, X.; Hratchian, H. P.; Izmaylov, A. F.; Bloino, J.; Zheng, G.; Sonnenberg, J. L.; Hada, M.; Ehara, M.; Toyota, K.; Fukuda, R.; Hasegawa, J.; Ishida, M.; Nakajima, T.; Honda, Y.; Kitao, O.; Nakai, H.; Vreven, T.; Montgomery, J. A.; Jr. Peralta, J. E.; Ogliaro, F.; Bearpark, M.; Heyd, J. J.; Brothers, E.; Kudin, K. N.; Staroverov, V. N.; Kobayashi, R.; Normand, J.; Raghavachari, K.; Rendell, A.; Burant, J. C.; Iyengar, S. S.; Tomasi, J.; Cossi, M.; Rega, N.; Millam, J. M.; Klene, M.; Knox, J. E.; Cross, J. B.; Bakken, V.; Adamo, C.; Jaramillo, J.; Gomperts, R.; Stratmann, R. E.; Yazyev, O.; Austin, A. J.; Cammi, R.; Pomelli, C.; Ochterski, J. W.; Martin, R. L.; Morokuma, K.; Zakrzewski, V. G.; Voth, G. A.; Salvador, P.; Dannenberg, J. J.; Dapprich, S.; Daniels, A. D.; Farkas, O.; Foresman, J. B.; Ortiz, J. V.; Cioslowski, J.; Fox, D. J. *Gaussian 09*, Revision B.01; Gaussian, Inc.: Wallingford, CT, 2010.

(36) Stephens, P. J.; Harada, N. *Chirality* **2010**, *22*, 229−233.

(37) Humphrey, W.; Dalke, A.; Schulten, K. *J. Mol. Graph.* **1996**, *14*, 33−38.

(38) Dennington, R.; Keith, T.; Millam, J. *GaussView*, Version 5; Semichem Inc.: Shawnee Mission, KS, 2009.